%\documentstyle[twocolumn,12pt,epsf,psfig,graphics,graphicx]{article}

HIGH TEST PEROXIDE HYBRID ROCKET RESEARCH

S. D. Heister, E. J. Wernimont and J. Rusek

July 24, 1998

Abstract

Results from 100 tests of labscale hybrid rocket motors using hydrogen peroxide and polyethylene are presented herein. The bulk of the tests utilized 85% peroxide with low density polyethylene. A new consumable catalytic ignition device has been utilized to provide rapid, reliable ignition using *stabilized* peroxide. Using this device, stable combustion has been initiated in both conventional and radial-flow hybrid rocket fuel geometries.

Introduction

Hybrid rockets are systems which have one propellant in solid form and the other in liquid form. Most applications utilize a liquid oxidizer with a solid fuel to enhance performance over the other alternative (solid oxidizer/liquid fuel). In the past few years, interest in hybrid rockets has increased due to the potential for these devices to reduce costs and enhance safety in aerospace propulsion devices. A variety of applications, including launch vehicle boosters, upper stage and tactical systems have been identified as areas in which hybrid propulsion concepts are of interest.

We can trace the use of the Hydrogen Peroxide (HP)/Polyethylene (PE) propellant combination to the mid 1950's.[1-3] While the early tests of Moore and Berman[1] were quite successful, interest waned (most probably due to the search for higher energy propellants during this era) and essentially no published work exists for a four decade period beginning in the mid 1950's. Current requirements for lower cost, non-toxic propulsion systems have motivated a renewed interest in this storable propellant combination. Recent efforts have been undertaken in our group,[4-9] at the University of Surrey in the United Kingdom[10] and the U.S. Air Force Academy.[11]

Recent system studies[4,5,12] point to potential benefits of HP-oxidized systems which include its high density, ease of handling, non-toxicity, and monopropellant characteristics. For example, both turbopump and pressurization systems can utilize decomposition energy and biproducts to effectively simplify engine power cycles and tank pressurization systems. In addition, the fact that HP hybrid systems tend to optimize at high mixture ratios provides a benefit in reducing the size of the expensive, high-pressure combustion chamber which contains the fuel grain. This benefit also decreases the sensitivity of these propellants to fuel slivering since the fuel provides a smaller fraction of the total propellant mass.

Polyethylene (PE) also represents a unique fuel choice in view of the fact that much of the present work focuses on the use of hydroxyl-terminated polybutadiene (HTPB) as fuel. While HTPB systems enjoy a slightly higher regression rate, which tends to reduce fuel grain complexity somewhat, this fuel is a thermoset compound which can only be produced using batch processing which necessitates substantial tooling capital investment, tooling assembly and disassembly. We suspect that the main impetus for the use of this chemical stems from the fact that most solid rocket manufacturers (many of whom also participate in hybrid rocket programs) commonly use this chemical in solid rocket propellants

In contrast to HTPB, PE is a thermoplastic which is commonly produced via extrusion from a die in a continuous process. Hence, PE grains could be produced using this approach by simply cooling the extruded product and cutting it to the desired length. Thermoplastics also eliminate waste since the product can be remelted if a part is made incorrectly. In addition, PE has a lower cost than HTPB and is much easier to machine even though the thermochemical combustion performance of the two materials is virtually identical. For these reasons, this material represents an attractive alternative for many missions.

For these reasons, an experimental program was initiated to quantify the combustion behavior of the HP/PE hybrid propellant combination. A unique consumable catalytic ignition system was used to provide the initiation of combustion in these studies. Factors considered in the tests described in this paper include: massflux, oxidizer/fuel (*OF*) mixture ratio, chamber pressure, fuel grain length (

%\documentstyle[twocolumn,12pt,epsf,psfig,graphics,graphicx]{article}

L^*), and PE formulation. The facility is briefly described in the following section, followed by a description of the ignition system, and experimental results.

Test Apparatus/Methodology

This fluid system was designed to provide reliable combustion measurements with minimal complexity and redundant safety features. To this end, a simple cartridge-loaded combustion chamber is utilized with a simple "nozzle" designed to provided the required throat area without an exit cone (simple throat plug). Figure 1 highlights the 2 inch outside diameter combustion chamber design; the catalytic ignition device is described in detail in the following section. The insulating materials used for these tests are paper phenolic. The nozzle material is a silica phenolic that provided a low erosion rate of less than 2.0 mils/sec for the configurations fired.

A schematic of plumbing and tankage associated with the test apparatus is shown in Fig. 2. This apparatus provides for safe firing of a hydrogen peroxide hybrid rocket motor by remote operation from a concrete enclosed control room. The entire fluid system utilizes materials compatible with high-concentration hydrogen peroxide such as 300-series stainless steels, glass and teflon. The high pressure HP tank is pressurized using a Nitrogen "K-bottle" with manual isolation valve, MV1, depicted in Figure 2. A second K-bottle (manual isolation valve MV4) is used to provide high pressure gas for remote actuation of stainless steel pneumatic valves denoted PV1 and PV2 in Fig. 2. The fluid is loaded by opening valve MV3 and pouring the liquid through a funnel into the oxidizer tank. During a test, the system is operated by simply opening the main oxidizer valve (PV1) until all of the HP loaded in the oxidizer tank is consumed. Gaseous nitrogen is then driven into the combustion chamber causing quenching of the remaining fuel.

As can be seen from Fig. 2, this system incorporates many safety features. Actuation of pneumatic valve PV2 provides for dumping and dilution of the HP (PV2) in the event of an emergency. During the entire test program, there were no occasions in which dumping of the HP was required. Other safety features include: a normally-open venting solenoid valve (SV2), a remotely-actuated manual vent valve (MV5), and a relief valve (RV1) on the oxidizer tank. These features were installed to allow venting of the oxidizer system in the event that undesired decomposition of the loaded HP occurs.

Instrumentation for these tests consist of ullage and chamber pressure, oxidizer turbine flow meter information as well as axial thrust measurement. This set of information (plus pre/post-test fuel grain measurements) is sufficient to determine motor operating parameters as well as information on fuel regression rate. Digital data acquisition is achieved through the use of a Pentium-based PC with a Keithley/Metrabyte analog/digital converter. This data acquisition system is used to real time display the conditions of oxidizer tank temperature (T1) and pressure (P3) during HP loading. This provides a means of determining if an emergency dumping procedure must be conducted if the loaded HP is unstable in the tank.

During a firing the data acquisition system is used to sample the motor operation parameters at 250 Hz per instrument. In each test, oxidizer flow rate is held approximately constant using the self-limiting combustion behavior of hybrid rocket motors. i.e., the rate of oxidizer injected into the combustion chamber is a direct function of the ullage-to-chamber pressure differential and the chamber pressure is also dependent on the oxidizer flowrate (for given nozzle and fuel port diameters). Assuming no throat erosion, both chamber pressure and oxidizer flow rate may be held constant by maintaining a constant ullage pressure. Constant ullage pressure is achieved by regulated nitrogen pressurant gas. This technique is used for all the tests presented in this paper.

The test program was formulated to maximize the amount of information available to actually design a HP/PE hybrid. For this reason, many different parameters were studied, none of which were studied in tremendous detail. Most parameters were investigated across a range of total mass port flux levels allowing determination of fuel regression rate influence. The entire test program involved firing eleven different series of motors, with each series dedicated to examination of a specific parameter. A total of 100 firings were conducted in association with these test series which are summarized in Table 1. With the exception of the C-Series tests (which will be described in the Test Results section), all motors used the combustion chamber design shown in Fig. 1. The following sections will discuss results obtained from these tests.

Table 1: Test Series Summary

Series	Purpose	Number of Motors	Test Parameters
A	System Verification	12	$\tilde{P}_c \sim 100\,\mathrm{psia}$

%\documentstyle[twocolumn,12pt,epsf,psfig,graphics,graphicx]{article}

			$\overline{G}$ 0.25 to 0.35 $lb_m/(in^2-s)$
			85% HP Interox, HDPE
B	Broader Flux	12	$\overline{G}$ 0.15 to 0.35 $lb_m/(in^2-s)$
			Three at 80% HP Interox
C	Radial Flow Motor	20	Proof of Concept
			8 Ignition Tests
D	Polyethylene Types	11	LDPE, UHMW
E	Higher Mass Flux, P_c	8	Flight Weight, LDPE
			Proof of Combustion
F	New HP Vendor	5	Air Liquide 85%
G	Increase P_c		
H	Lengthen Aft Combustion	4	Increase by 2, 4 Inches
I	Action Time Study	4	Two at 6, 9 Seconds Each
J	Increase P_c		$\tilde{P}_c \sim 400$ psia
M	Increase Mass Flux	1	G 0.35 to 1.0 $lb_m/(in^2-s)$
Y	Ignition Behavior	4	Visual Observations, PMMA Fuel

HTP Usage in Test Program

Because concentrations no greater than 70% were domestically available for the majority of this project, it was necessary to concentrate much of the fluid used in this research. During the first portion of the tests conducted under this research, the 80 to 85% HP was made via concentration of stabilized Interox 50% HP. To concentrate HP, several methods are available that make use of the differences in vapor pressure or the freezing point between water and anhydrous HP. Open air boiling was selected because this method is simple and requires a minimum of equipment. This method operates under the principal that the vapor pressure for HP is lower than that of water, in which case the boiling water/HP fluid will preferentially drive off the water.

For concentration from 50% to 85% the boiling begins around 225 F and terminates at 280 F. At such an elevated fluid temperature, only glass containers may be used without spontaneous combustion. This method may only be used with highly stabilized HP because a self-consuming thermal decomposition wave is formed in the liquid for unstabilized HP above 70% concentration.[13] The decomposition wave can be set up in stabilized fluid as one reaches concentrations above 90%. In some instances, the energy from a vapor-phase detonation in the gases above the boiling surface did initiate a thermal decomposition wave during this research program. While these vapor-phase detonations were not terribly energetic (many of them sounded like a small firecracker exploding), some were strong enough to crack/shatter the flasks used for boiling in this study. We were able to capture one instance of thermal decomposition on film; from this footage we estimate that the wave speed is about 1 cm/s. We presume the detonations were initiated by small amounts of airborne debris or particulate contamination on the surface of the flask. Since the primary goal of this research was not aimed at understanding the concentration process, these issues were not pursued in detail.

Concentration from 50% was performed by remote heating in 4000 ml Erlenmeyer flasks until a batch of 4 to 5 gallons of 85% is manufactured. This is done to minimize variations of fluid physical properties on the fired motor data. Concentration by this method also concentrates the stabilizer in the original fluid. Later in the test program (after 55 motors), unstabilized HP was purchased from Air Liquide in France at 85% concentration. This fluid is then stabilized to the desired amount by addition of sodium stannate and phosphoric acid (see Table 2). The stabilizer level selected for the Air Liquide HP is around one half that produced by open air boiling of the Interox fluid. This is done to determine if fuel regression is greatly effected by reduced stabilizer level.

Table 2 shows the batches used and the stabilizer level as well as the actual concentration as tested by Rusek.[14] As a reference, the maximum allowable stabilizer level for U.S. Military Specification[15] is provided in the table. The MilSpec is intended for fluid to be

used in silver screen catalytic beds; in this application the stabilizer can attack the bed material and therefore must be tightly controlled. Since we employ a consumable catalytic bed (see next section), our devices were not sensitive to stabilizer level. The table shows that the fluid used in this test program had stabilizer levels over 100 times higher than that permitted in the MilSpec.

Table 2: Hydrogen Peroxide Concentration and Stabilizer Level

Batch	Concentration	Phosphorus	Tin	Sodium
	wt %	(ppm)	(ppm)	(ppm)
A	85.7	36.3	48.8	53.8
B	80.7	29.8	40.6	43.7
C	86.9	36.2	47.1	54.1
M	85.0	38.2	40.7	Not Tested
AL	84.1	11.7	24.3	Not Tested
US Mil Spec	90.0	0.2	4.0	NA

Consumable Ignition Device

Probably the greatest challenge in creating a workable hybrid propellant combination lies in the development of an ignition concept which provides a rapid and reproducible rise in chamber pressure and thrust. In the past, secondary injection of pyrofuoric fluids, electric ignition sources, torches, and catalytic ignition systems have been used in hybrid rockets. With the exception of the catalytic system, all these concepts require additional hardware and/or fluids to support ignition of the motor. For this reason, the catalytic concept was pursued through the use of a consumable catalytic bed (CCB). While catalytic devices such as silver screens and other materials treated with catalytic material have been used to decompose peroxide in the past,[16] the present concept[17] provides several advantages over these techniques:

- The CCB concept supports operation with *stabilized* HP (successful tests with stabilizer levels as high as 50 ppm). Mostof the previous systems could not operate with stabilizers (primarily stannate and phosphate compounds) in the fluid because these materials would reduce the catalytic activity of the bed material. Use of stabilized fluid throughout this test program has been viewed as a substantial safety enhancement.
- The CCB provides an energetic ignition system with no inert parts, thereby maximizing the propellant mass fraction of the propulsion system.
- Since the device requires no inert hardware (or other fluids/gases) it also represents a minimum cost ignition system.

The CCB is inserted into a pocket which was machined into the forward end of the fuel grain as noted schematically in Fig. 1. No special ignition sequence was utilized in any of the testing, the engine was literally "slam started" by opening valve PV2 (see Fig. 2) which provides maximum HP flow. As HP passes through passages in the CCB it is decomposed. If the HP is at sufficient concentration, the decomposition products are at a temperature such that autoignition of the PE occurs. As the HP flow continues, the CCB is consumed. If the CCB is sized properly, there will be enough energy in the combusting fuel grain to support thermal decomposition of the HP injected after CCB consumption; i.e. the device operates for only a small fraction of a firing.

Figure 3 highlights a group of typical ignition transients obtained with the use of 85% HP in the design. This collection shows that the CCB is repeatable and produces rapid ignition transients. The peaks at approximately 30 msec represent a pressure overshoot due to increased oxidizer mass flow when the oxidizer valve is first opened. Because there is no cavitating venturi in the fluid system, the oxidizer mass flow is governed strictly by pressure differential. Consequently, initial fluid flow is greatest for the first 20 msec before the chamber pressure has a chance to climb to its steady state value. As can be seen from the figure, steady-state combustion has been achieved in 50 msec.

To aid in the understanding of the rate of consumption of the device, a series of four motors (Y-series in Table 1) were fired using transparent acrylic, (PMMA) fuel grains. Still photographs were taken during these firings; a typical set of images noting CCB consumption is shown in Fig. 4. The photos were taken with the auto-iris set on the camera so intensity levels are not necessarily representative of temperature. In this Fig 4., the CCB is on the right and flow is from right to left. At ignition (t=3.3 sec), the fuel port is already luminous indicating reaction within the CCB. The second image, taken just prior to the chamber pressure decrease, shows complete consumption of a small portion of the CCB at one circumferential location. In the next frame available from the camera (t=5.5 sec) the entire aft portion of the CCB has been consumed or expelled from the motor. This event correlates well with a small decrease in chamber pressure in the motor; this behavior was noted frequently in the testing program.[18]

The final image, taken just prior to total oxidizer consumption (t=11.5 sec) shows a small dark region at the head-end of the grain. Since postfire inspection revealed that the entire CCB had been consumed (or expelled), this dark region corresponds to the zone in which HP decomposition occurs. Postfire fuel samples are in agreement with this theory; negligible regression is observed in this region.

Test Results

As indicated in Table 1, a broad range of tests were conducted over the twelve test series. While the HP stabilizer levels varied substantially through the course of the testing, there were minimal combustion variations attributed to this factor. The Air Liquide fluid with the lower stabilizer levels appeared to cause a bit more fuel consumption in the CCB area; perhaps the reduced stabilizer level served to enhance CCB consumption, but the chamber pressure traces did not particularly support this theory. Early efforts were aimed at optimizing fuel grain length so as to obtain *OF* ratios near the 7.5 value which tends to maximize specific impulse for these propellants. Many of the later tests actually achieved fairly low mixture ratios (in the 5-6 range) due to the fact that fuel regression rates exceeded our estimates. A complete tabulated list of all test conditions can be found in Ref. 18; we will not include all these data here in the interest of brevity.

Reliable ignition and combustion was demonstrated over a range of initial oxidizer fluxes $0.1 < G_{ox} < 1.2 \mathrm{lb}_m/(\mathrm{in}^2 s)$ and chamber pressures $100 < P_c < 400$ psia during the testing with 85% HP. A few tests were conducted with 80% HP, but reliable ignition and combustion could not be achieved using the injector and CCB design implemented in these tests. We believe that one could design a device to operate at these lower concentrations with an improved injector (with smaller droplet sizes) and CCB designs. Our injector produced droplets which were quite large, a 350 micron volumetric mean diameter is reported by the manufacturer. Limited information[18] suggests that ignition and combustion at concentrations lower than 80% would be very difficult for PE; at these concentrations most of the decomposition energy goes into vaporizing the water in the aqueous HP. Here we should note that concentrations below 67% have insufficient decomposition energy to vaporize water within the mixture.

Axial-Flow Test Results

The bulk of the testing involved the conventional combustion chamber design shown in Fig. 1. An image of a typical firing at a chamber pressure of roughly 200 psi is shown in Fig. 6. Note that the plume is nearly transparent when high combustion efficiency is achieved; the main source of luminosity is from the particles of throat and insulation material radiating within the plume itself. Typical chamber pressure histories obtained during the test program are shown in Fig. 6. Overall, the combustion obtained was very smooth as evidenced by the low amount of noise in the pressure signals. Typical unsteadiness in the pressure signals was of the order of 1-2% (zero-to-peak) of the mean pressure in this test program. Sharp tailoffs were always observed in the testing commonly used in solid rocket data reduction. The spike in the motor F4 and H3 traces in the interval $1 < t < 2$ seconds is attributed to ejection of small portions of the CCB through the nozzle. In the M1 pressure trace, a slight increase in P_c is observed after the main ignition event. This behavior may be attributed to increased oxidizer flow rate due to a change in injector discharge coefficient.[18]

While there were test series dedicated to assessing the influence of PE type on fuel regression and combustion, the bulk of the measurements were obtained using Low Density PE (LDPE) fuel. A compilation of these measurements is provided in Fig. 7 which highlights dependence of regression rate on *both* flux level and chamber pressure and compares our results with those of other researchers. Mass addition from the CCB necessitated our development of a new data reduction scheme[19] for hybrid rockets; this scheme was used to determine average regression

rates in the axial-flow studies. While the low pressure (100 psi) data appear to behave a classical regression law $(r \propto G^n)$ consistent with diffusion-dominated behavior, the higher pressure results show a distinct insensitivity to port total mass flux (G) in the range $0.1 < G < 0.3 \mathrm{lb}_m/(\mathrm{in}^2 s)$. In this lower flux region, regression rates at the higher pressures tested (200 and 400 psia) are as much as 75% greater than those at low pressures. The data are consistent with a radiation-based regression law which has been theorized, but infrequently observed for low massflux conditions.

In fact, this behavior is ideal since regression rates would no longer be influenced by changes in port geometry (either shape or size). For the booster application, design studies[5] indicate an optimal massflux level of about $0.4\ lb_m/(in^2 s)$ assuming a classical regression law, $r \propto G^{0.8}$. Presumably, designers could make use of this desirable behavior (flux insensitivity) for other applications as well.

To compare the data from this test program with that of previous researchers,[1-3,20,21] we performed correlations assuming a classical, massflux-dominated regression behavior. While this approach is not warranted for the higher pressure results, it does permit gross comparisons with results of other researchers who made similar assumptions. The resulting correlations are presented in Table 2. Note that for the low pressure data the exponent of 0.78 is in close agreement with theory assuming a diffusion-dominated behavior. The exponent is reduced at the higher pressures due to the radiative-dominated behavior. In general, the results from our studies are in agreement with the GE data, but we observe slightly higher regression rates at all flux levels than those measured by Moore and Berman.

Table 3: Summary of LDPE/85% HP Fuel Regression Flux Correlations

Correlation	$\overline{P_c}$	$\overline{G}$
0.040 $G^{0.78}$ ips	100 psia	0.1 - 0.3 $lb_m/(in^2 - s)$
0.035 $G^{0.52}$ ips	200 psia	0.1 - 0.3 $lb_m/(in^2 - s)$
0.041 □ ips	400 psia	0.2 - 0.7 $lb_m/(in^2 - s)$

Numerous other test data were obtained in this portion of the research program; in the interest of brevity we will simply highlight these results. Combustion efficiencies above 95% were attained routinely in this testing; results showed substantial gains in efficiency were obtained by using a mixing section at least 4 inches (two chamber diameters) in length. These aft mixing volumes are consistent with characteristic chamber lengths (L^*) of about 40 inches. Here, we compute L^* as the combustor volume aft of the fuel grain and forward of the throat divided by the throat area. The L^* value of 40 inches is typical of bipropellant liquid engines using hydrocarbon fuels.

Substantial efforts were also expended to quantify the level of combustion stability in these test firings. As noted in the discussion of Fig. 6, there were no notable combustion instabilities in this test program. Recent theoretical efforts[22] suggest that thermal lags in the fuel can account for the low-frequency (1-100 Hz) oscillations which have been observed in numerous tests which have used either liquid or gaseous oxygen as the oxidizer. In contrast to liquid oxygen systems which tend to optimize at *OF* values near 2.5, the HP/PE system optimizes at much higher *OF* ratio (typically around 7.5). In this case, the mass and energy addition from the fuel is much less than in oxygen oxidized systems, thereby reducing the overall amplitude achievable. This factor may explain our distinct lack of instabilities. However, we should note that all testing was performed on a fairly small scale apparatus (2 inch diameter fuel grain) and additional larger scale work will be required to confirm this suspicion.

Radial-Flow Test Results

As noted in the previous section, a series of tests (C-Series in Table 1) were dedicated to a unique, radial-flow geometry in the fuel section. A schematic of the combustion chamber used in these tests is shown in Fig. 8. The radial-flow design permits the use of large burn surface areas and thrust levels without the complication of manufacturing multiport grains. In addition, this geometry permits the design of very short propulsive stages. Primary applications include upper stage systems and boost systems for launch vehicles.

Our particular test geometry (Fig. 8) resulted from several compromises aimed at reducing costs and possibility of catastrophic failures. The combustion chamber was fed by an initially axial flow in which a CCB device such as that described in the previous section was utilized. A substantial amount of testing was performed to insure that rapid, reproducible ignition could be obtained in the unique

combustion chamber geometry.[23,24] The design rationale was to insure that the HP was decomposed prior to the radial passage between the fuel plates; i.e. the design avoided possible pooling of the HP on the lower fuel disk during startup. While an annular throat might be attractive for a "pancake motor" design such as this, we chose to utilize seven conventional throat plugs to provide the necessary throat areas during the testing. An image of a typical test is shown in Fig. 9 which highlights the flow from each of the seven throat locations.

Because the throat plugs are of small initial radius, throat erosion led to significant decay in the chamber pressure histories as indicated in Fig. 10. In this figure, we have overlaid chamber and ullage pressure histories from three different firings (C7,C8,C9) which were designed for burning times of about 5, 10, and 15 seconds respectively. Here, the target chamber pressure was 100 psi. Note that the actual chamber pressures were well above this target indicating that actual burning rates exceeded our estimates. Also note the reproducibility of the chamber pressures over the first six seconds common to each of the three tests. In addition, the overall "noise" in the pressure traces are quite low and within the range of $\pm 5\%$ generally considered for smooth combustion.

A large number of measurements were made to determine the postfire fuel plate geometries for each of the full duration tests. A typical set of results from these measurements is shown in Fig. 11 for test C5. Here, postfire fuel section geometries are shown along 14 rays equally-spaced azimuthally. On the upper fuel plate, only minor azimuthal variations are noted, whereas the lower plate exhibits more scatter, especially in the center of the plate which is subjected to impingement from the axial jet of HP decomposition products. In this particular test, which had a duration of 9.9 seconds, we actually see *less* fuel regression in this impingement region. Other testing at longer durations and higher chamber pressures indicates that this region can experience higher regression rates than neighboring regions.

The azimuthally-averaged fuel regression behavior for the three tests shown in Fig. 10 are depicted in Fig. 12. Here, we note a reasonably uniform regression behavior on the upper plate and on the outboard portion of the lower plate. This behavior indicates that efficient fuel utilization can result from this unique geometry. This conclusion is surprising since traditional hybrid rocket combustion theory would predict reduced regression on the outboard stations due to the increased flow area and decreased massflux levels at these locations. In fact, the flow between the disks is subject to an adverse pressure gradient and the possibility of flow separation due to the increased flow area at greater radial distances from the centerline. We did not see any evidence of gross flow separation, and the relatively uniform regression behavior indicates a radiative heat transfer mechanism, rather than the convective-dominated flows observed in most hybrid rockets. If this theory is correct, one could design devices with much larger outer/inner radius ratios than were used in these particular tests.

Other testing was conducted to assess the effects of flux level and chamber pressure on the regression. Overall, the amount of regression did increase with flux level, but not to the extent predicted by classical combustion theory. Increased chamber pressure had very little effect on the upper fuel plate regression, but substantial changes in lower plate regression were observed (particularly in the flow impingement region). Changes in the initial gap between the plates (at fixed flux level) had little effect on upper plate regression, but did effect regression on the lower plate somewhat.

The regression data were averaged in the radial direction to determine the average regression rates on both upper and lower fuel plates. We caution the user that these data do not reflect important radial and azimuthal regression variations, but they do provide a means to determine the gross response of the combustion process to changes in flux level. Figure 13 presents a correlation of regression rate (in *in/s*) as a function of massflux level (in $lbm/in^2 - s$) for upper and lower fuel plates for each of the 10 full duration tests in this study. Results show that on average, the lower plate exhibits more regression and that both plates regression is correlated with *G*. The resulting correlations (shown in the figure) indicate a flux sensitivity below the theoretical exponent of 0.8; in particular the lower plate average regression responds more weakly to changes in flux level. In comparing these data to the axial-flow results (Fig. 7), at a flux level of 0.1 lbm/in^2 we see regression rates which are 2-3 times greater for the radial flow device (radial flow tests were conducted between 100 and 200 psi). This general result could be attributed to increased turbulence/mixing in the radial flow engine as compared to the conventional geometry.

Conclusions

This paper summarizes combustion measurements from testing of the hydrogen peroxide (HP)/polyethylene (PE) hybrid rocket propellant combination. The bulk of the tests utilized 85% HP with low density PE (LDPE), but some data are reported for other types of PE. A new consumable catalytic bed (CCB) design has been used to provide rapid, reproducible ignition using *stabilized* HP. Once

the CCB is consumed, the HP undergoes thermal decomposition as a result of exposure to combustion gases emanating from the ignited fuel grain. The device provides a simple, low cost (and weight) alternative for ignition of hybrid rockets.

Both conventional and radial-flow geometries have been tested. In the conventional geometry, measured regression rates indicate a classic diffusion-dominated behavior at chamber pressures of 100 psi, with flux exponents very near the theoretical value of 0.8. However, at higher pressures, radiation-dominated behavior in which regression appears to be insensitive to changes in flux. High combustion efficiencies (> 95 %) were obtained at the higher chamber pressure (200 and 400 psi) conditions by using aft mixing lengths equivalent to about two fuel grain diameters (4 inches). Smooth combustion was observed in all testing, with typical chamber pressure fluctuations in the range of 1-2% (zero-to-peak) of the mean. We speculate that the high mixture ratio (5-8) operation of this propellant combination plays a role in reducing the amount of energy available to drive nonacoustic instabilities.

Reliable, reproducible ignition was also achieved in radial-flow geometry. Results indicate reasonably uniform fuel regression on both upper and lower fuel plates, with the exception of the impingement region on the lower plate. While average regression rates do correlate with massflux levels, the spatial variations in massflux within the device do not seem to cause substantial local regression variations. This behavior may indicate a radiation-dominated situation. Overall, the regression in the radial flow geometry was greater than that of the conventional geometry at comparable flux levels.

References

[1] Moore, George E. and Berman, Kurt, "Solid-Liquid Rocket Propellant System," *Jet Propulsion*, Nov. 1965, pp 965-968.

[2] Moore, G. E., Driscoll, D. H., and Berman, K., "A Hybrid Rocket Propellant System: 90-Percent Hydrogen Peroxide/Solid Fuel; Part II," General Electric, Schenectady, N. Y., Technical Report R53A0509, July 1954.

[3] Moore, G. E., Driscoll, D. H., and Berman, K., "A Hybrid Rocket Propellant System: 90-Percent Hydrogen Peroxide/Solid Fuel; Part I, General Considerations," General Electric, Schenectady, N. Y., Technical Report R52A0516, July 1954.

[4] Ventura, M. and Heister, S. D., "Hydrogen Peroxide as an Alternative Oxidizer for a Hybrid Rocket Strap-on Booster," *Journal of Propulsion and Power*, V. 11, No. 3, pp. 562-565, 1995.

[5] Vonderwell, D. J., Murray, I. F., and Heister, S. D., "Optimization of Hybrid Rocket Engine Fuel Grain Design," *Journal of Spacecraft and Rockets*, V 32, No. 6, pp. 964-969, 1995.

[6] Wernimont E. J., Meyer S. E., "Hydrogen Peroxide Hybrid Rocket Engine Performance Investigation," AIAA 94-3147, 30th Joint AIAA Propulsion Conference, Indianapolis, IN, June 27-29, 1994.

[7] Wernimont, E. J. and Heister, S. D., "Performance Characterization of Hybrid Rockets Using Hydrogen Peroxide Oxidizer,'" AIAA Paper 95-3084, 31st AIAA/ASME/SAE/ASEE Joint Propulsion Conference, San Diego, CA, July, 1995.

[8] Wernimont, E. J. and Heister, S. D., "Progress in Hydrogen Peroxide Oxidized Hybrid Rocket Experiments," AIAA Paper 96-2696, 32nd AIAA/ASME/SAE/ASEE Joint Propulsion Conference, Lake Buena Vista, FL, July, 1996.

[9] Wernimont, E. J., and Heister, S. D., "Experimental Study of Chamber Pressure Effects in a Hydrogen Peroxide-Oxidized Hybrid Rocket," AIAA 97-2801, 33rd AIAA Joint Propulsion Conference, 1997.

[10] Sellers, J. J., "Investigations into Hybrid Rockets and Other Cost Effective Propulsion Options for Small Satellites," Ph.D. Dissertation, University of Surrey, 1996.

[11] Humble, R. and Sandfry, R., "HYSTAR Hybrid Rocket Program at the United States Air Force Academy," AIAA 97-2797, 33rd AIAA Joint Propulsion Conference, 1997.

[12] Clapp, M.B. and Hunter, M.W., "A Single Stage to Orbit Rocket with Non-Cryogenic Propellants," AIAA 93-2285, 29th AIAA Joint Propulsion Conference, 1993.

[13] Wrobel, W., Orbital Sciences Corporation, Personal Communication, March, 1996.

[14] Rusek, J., China Lake Naval Weapons Center, Personal Communications, September, 1996 and February, 1997.

[15] Military Specification: Propellant, Hydrogen Peroxide, United States Air Force, MIL-P-16005E, Notice 1, 20 June 1988.

[16] Rusek, J. J., "New Decomposition Catalysts and Characterization Techniques for Rocket-Grade Hydrogen Peroxide," *Journal of Propulsion and Power*, V 12, No. 3, 1996.

[17] Wernimont, E. J., and Meyer, S. E., and Ventura, M. C., "A Hybrid Motor System with a Consumable Catalytic Bed, A Composition of the Catalytic Bed and A Method of Use," U.S. Patent Application No. 08/623,937, Filed March 28, 1996.

[18] Wernimont, E.J., "Experimental Study of Combustion in Hydrogen Peroxide Hybrid Rockets," Ph.D. Thesis, Purdue University, 1997.

[19] Wernimont, E.J. and Heister, S.D., "A Reconstruction Technique for Reducing Hybrid Rocket Combustion Test Data," *Journal of Propulsion and Power*, In Review, 1997.

[20] Pugibet, M. and Moutet, H., "On the Use of Hydrogen Peroxide as Oxidizer in Hybrid Systems," *La Recherche Aerospatiale*, No. 132, No. 132, 1969, pp. 15-31. Translated From French by NASA as TTF-13034, May, 1970.

[21] Osmon, R. V., "An Experimental Investigation of a Lithium Aluminum Hydride-Hydrogen Peroxide Hybrid Rocket," *Aerospace Chemical Engineering*, Vol. 62, No. 61, No. 61, 1966, pp. 92-102.

[22] Karabeyoglu, M. and Altman, D., "The Transient Behavior of Hybrid Rockets," AIAA 97-2937, 33rd AIAA Propulsion Conference, 1997.

[23] Caravella, J. R., Heister, S. D., and Wernimont, E. J., "Characterization of Fuel Regression in a Radial Flow Hybrid Rocket," *Journal of Propulsion and Power*, V14, 1, pp 51-56, 1998.

[24] Caravella, J. R., "Experimental Investigation of Combustion in a Radial Flow Hybrid Rocket Engine," M.S. Thesis, Purdue University, 1996.

Figure 1: Cross Sectional View of the Combustion Chamber

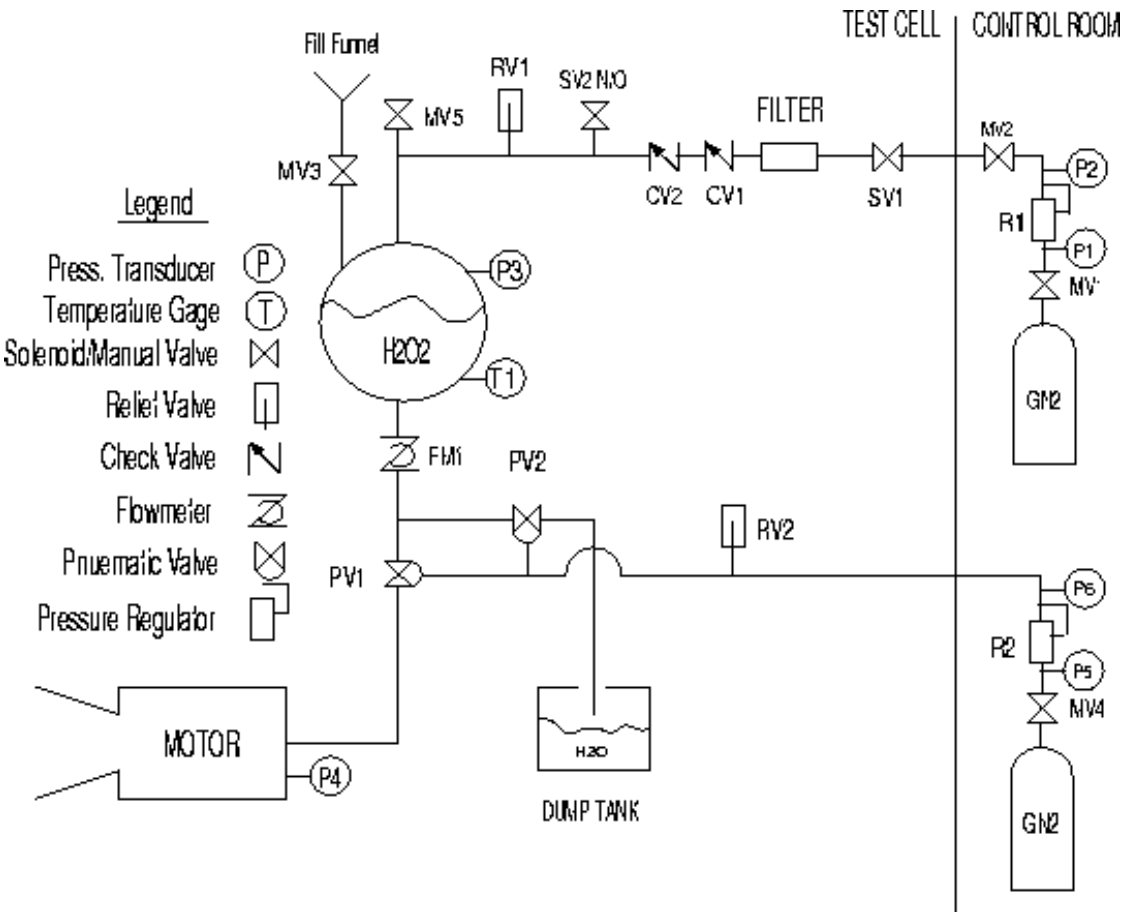

Figure 2: Test Facility Schematic

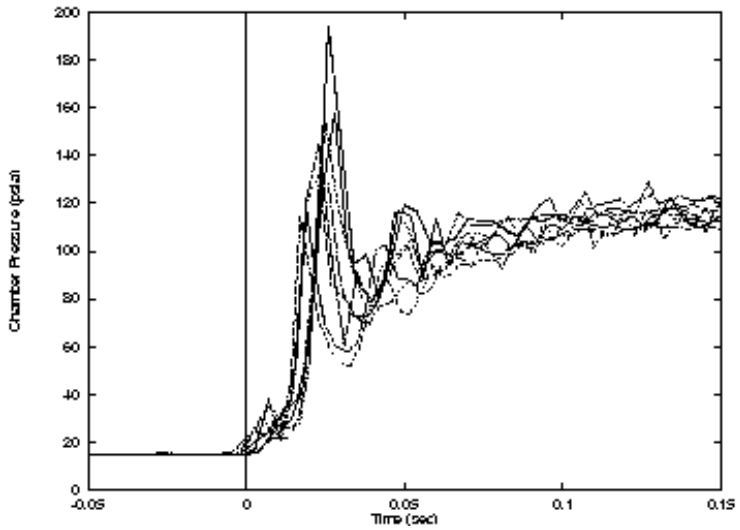

Figure 3: Typical Motor Ignition Traces (from D-Series Testing)

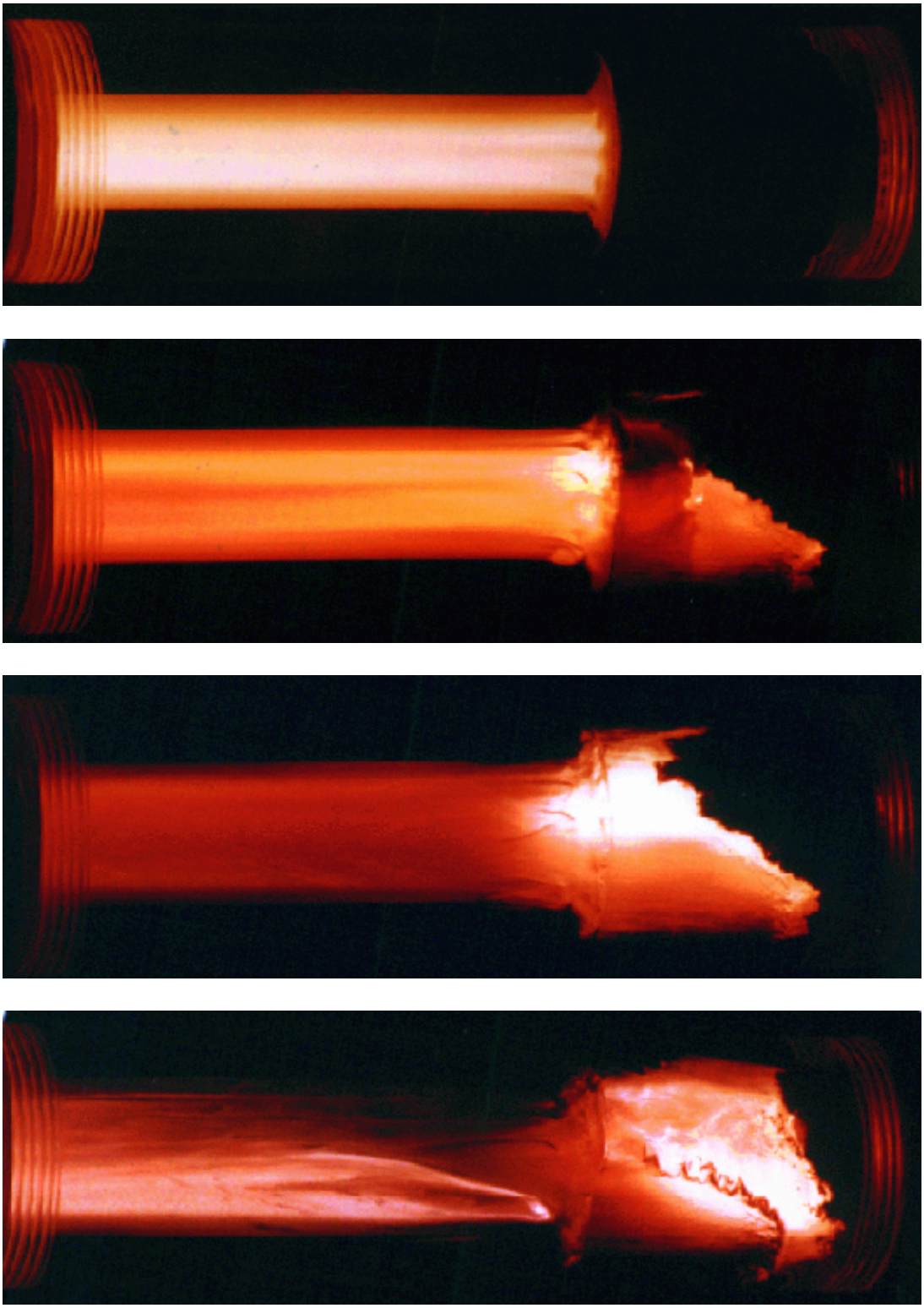

Figure 4: Still Photographs of Motor Y1 showing CCB consumption. Here, the CCB is located on the right hand side of the image and flow is from right to left. From top to bottom, images are for t = 3.3, 5.45, 5.5, and 11.5 sec.

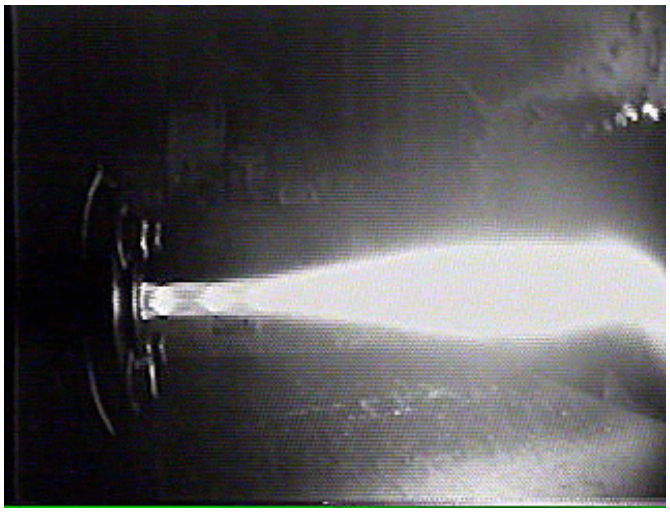

Figure 5: Image of Typical Engine Firing (Test G2)

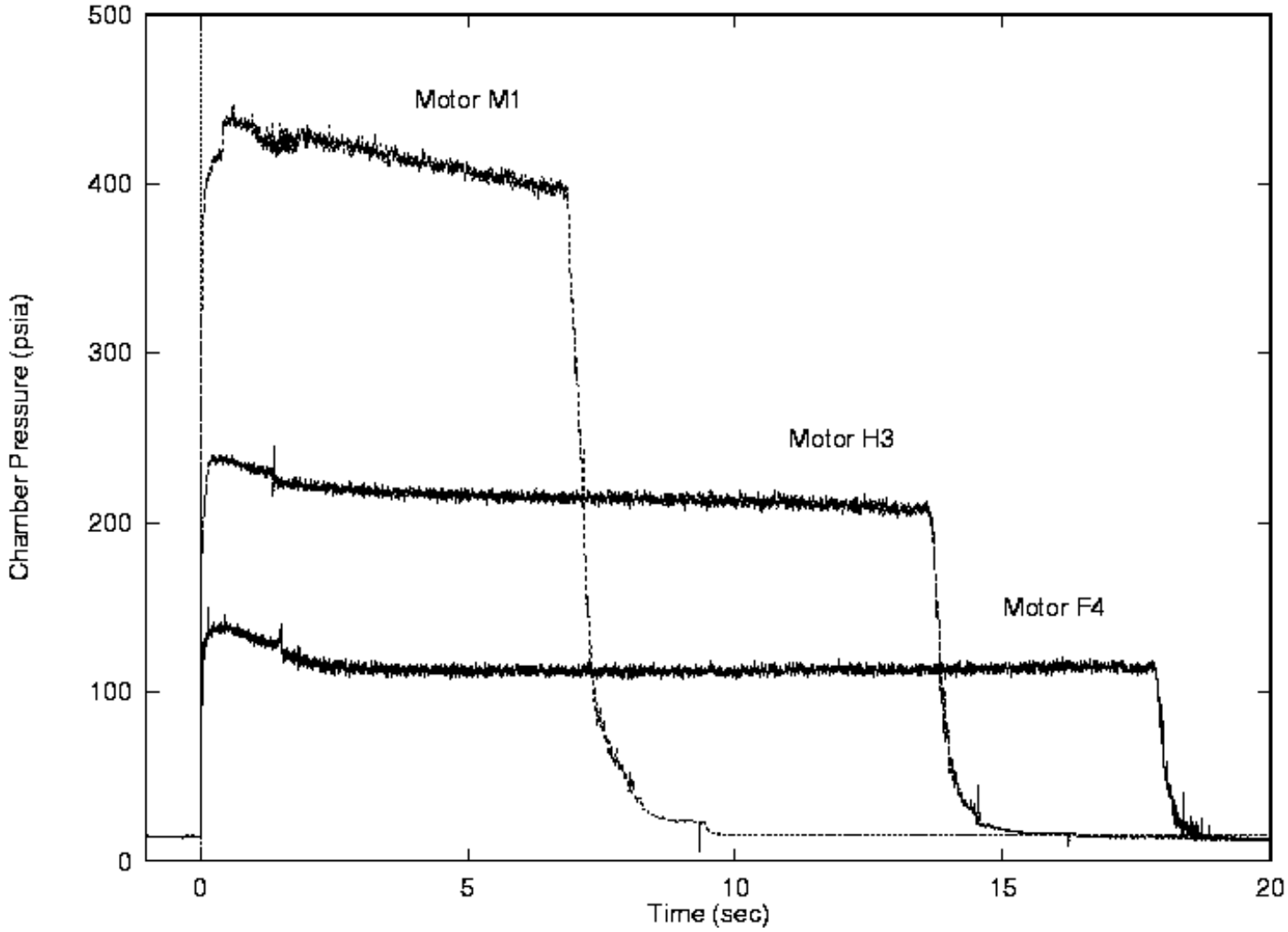

Table 6: Measured Chamber Pressure Histories for Motors F4, H3, and M1 at Average Pressures of Roughly 100, 200, and 400 psi, Respectively

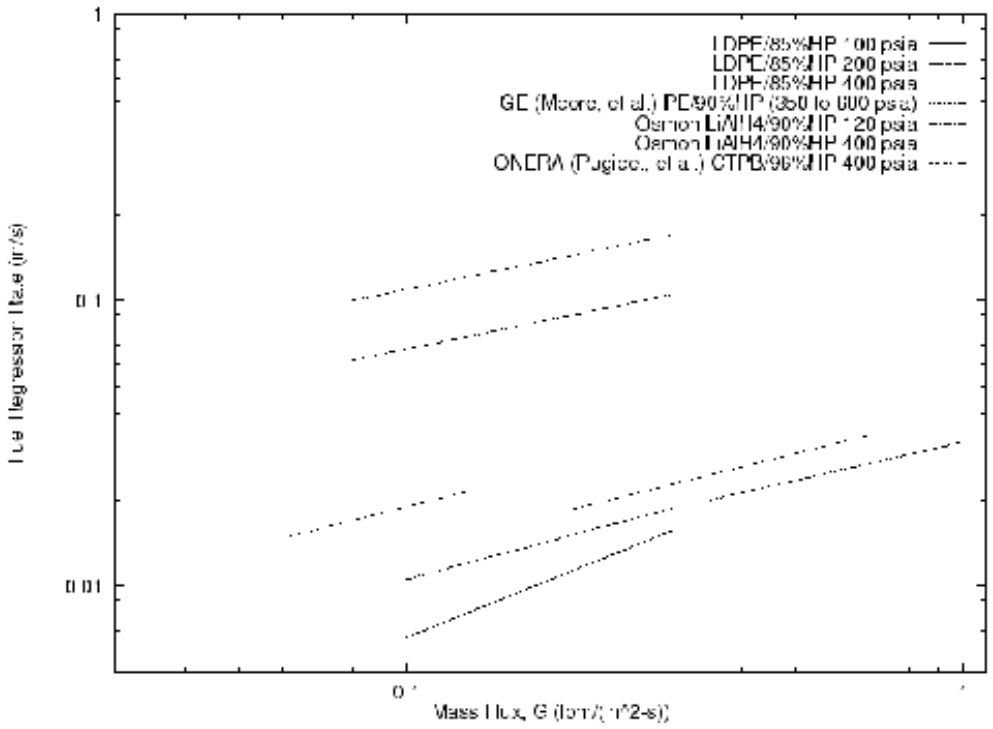

Figure 7: Comparison of Previous HP Investigators Regression Rate Measurements to Present Study

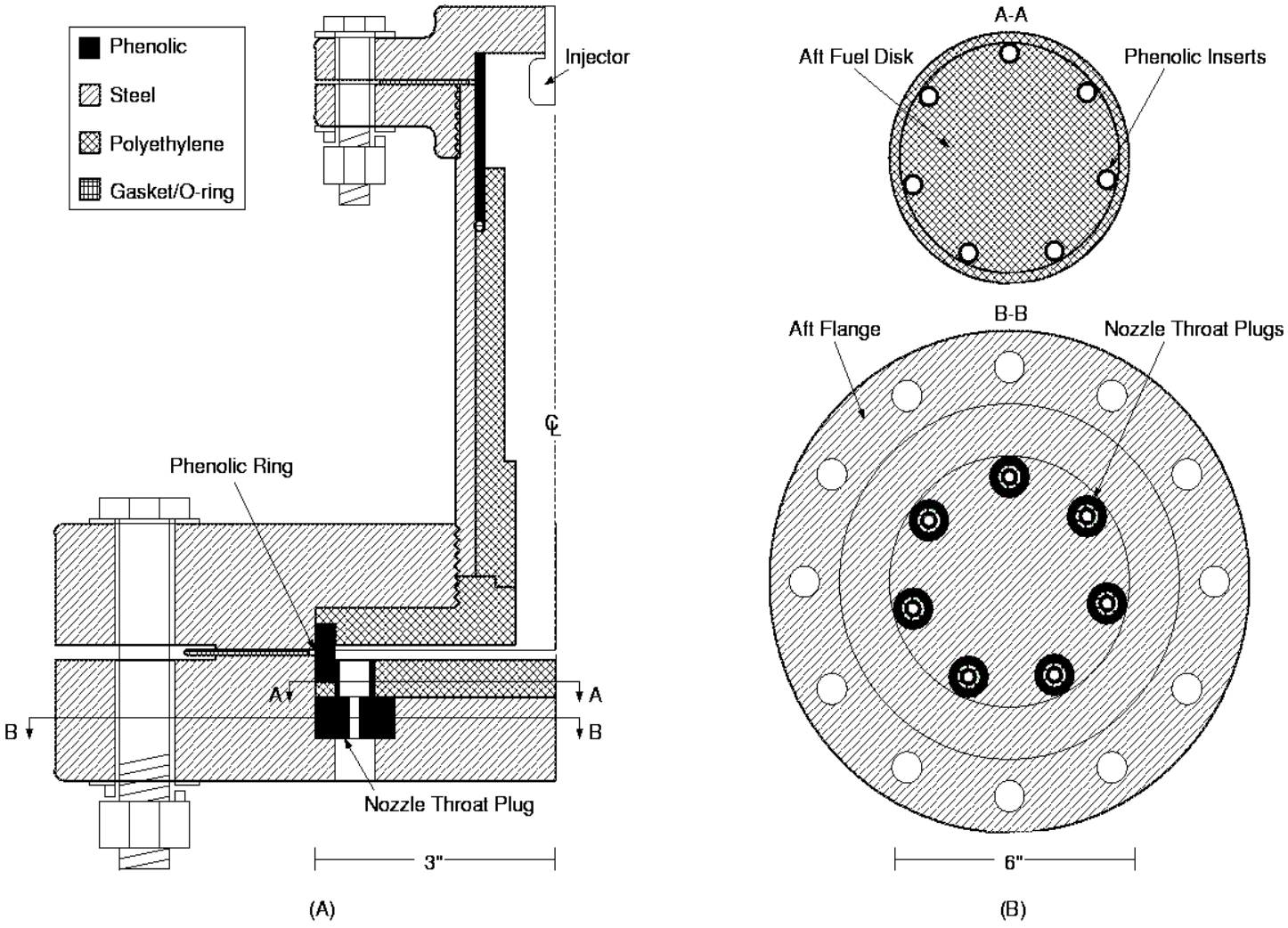

Figure 8: Radial Flow Test Engine Design

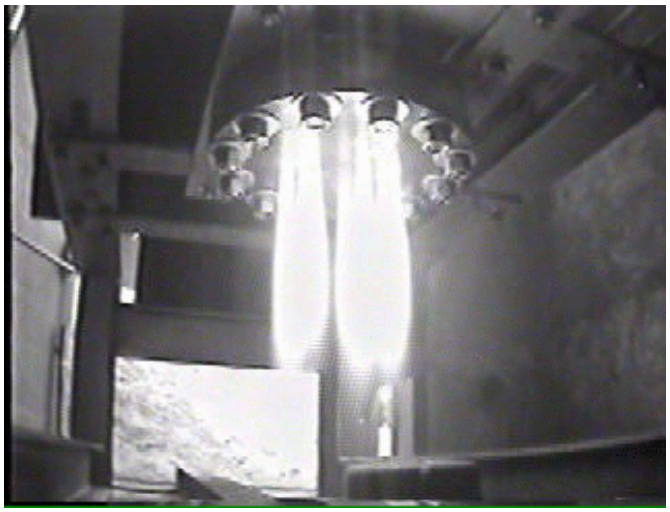

Figure 9: Image of Typical Radial-Flow Engine Firing (Test C10)

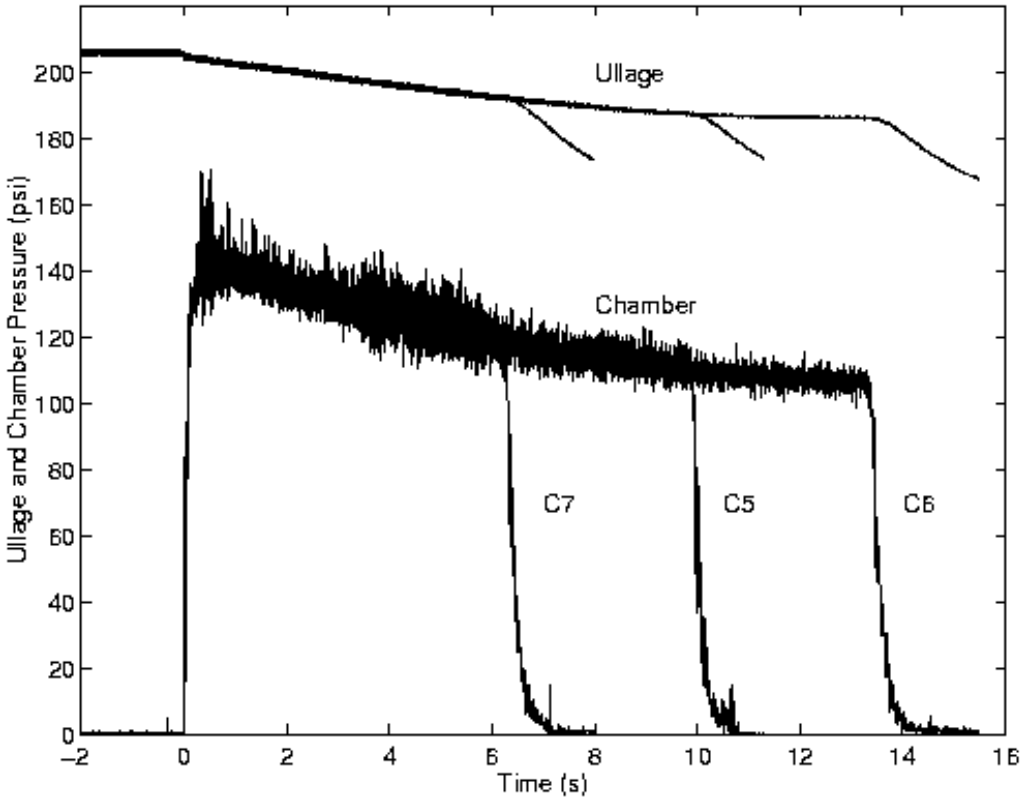

Figure 10: Chamber and Ullage Pressure Histories, Tests C5, C6, and C7

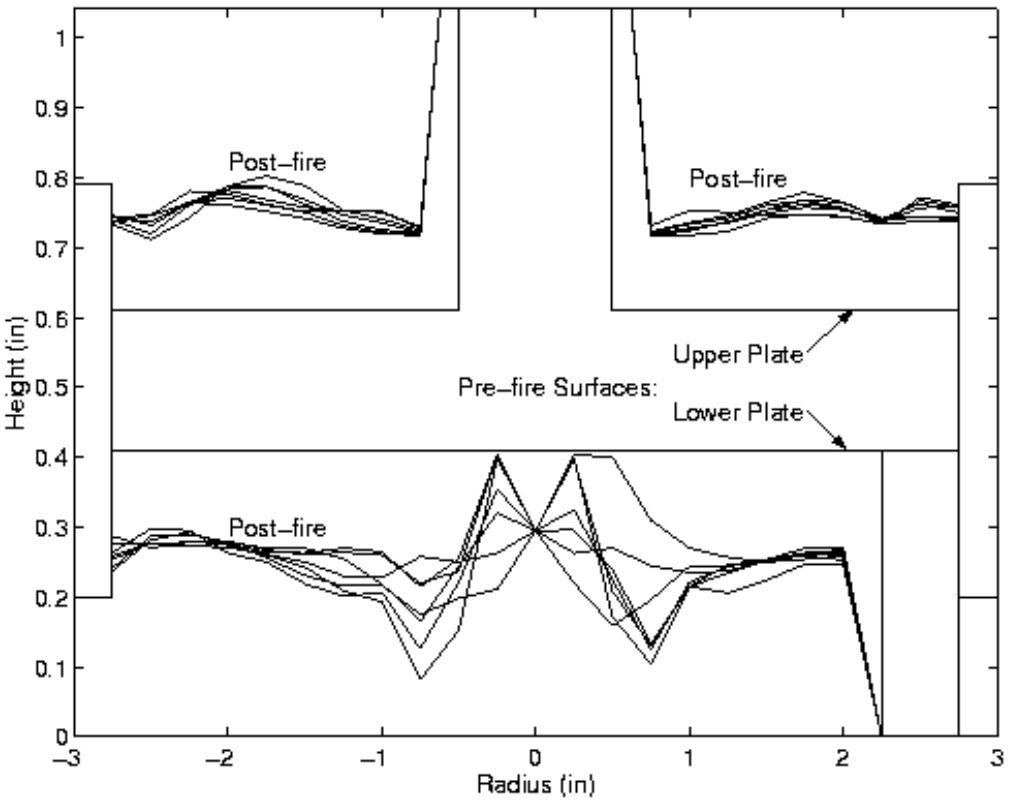

Figure 11: Azimuthal Variation in Surface Regression, Test C5

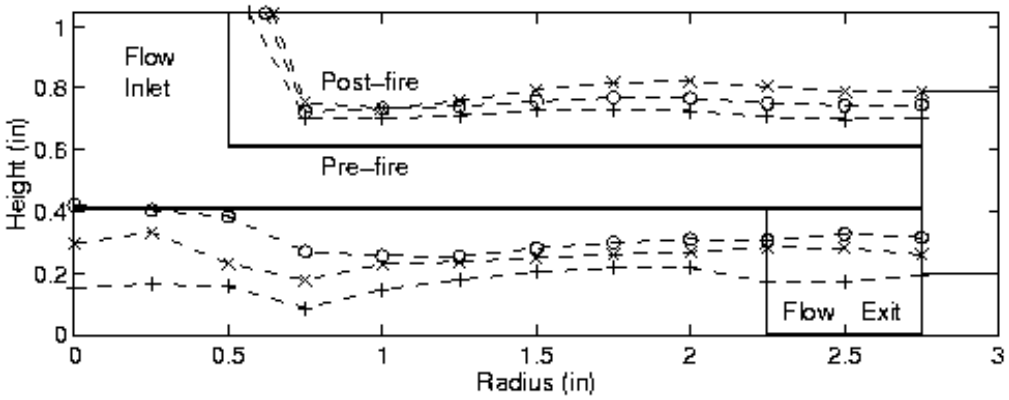

Figure 12: Azimuthally-Averaged Geometry (Pre-fire and Post-fire) for Tests C6 (o), C5 (x), and C7 (+)

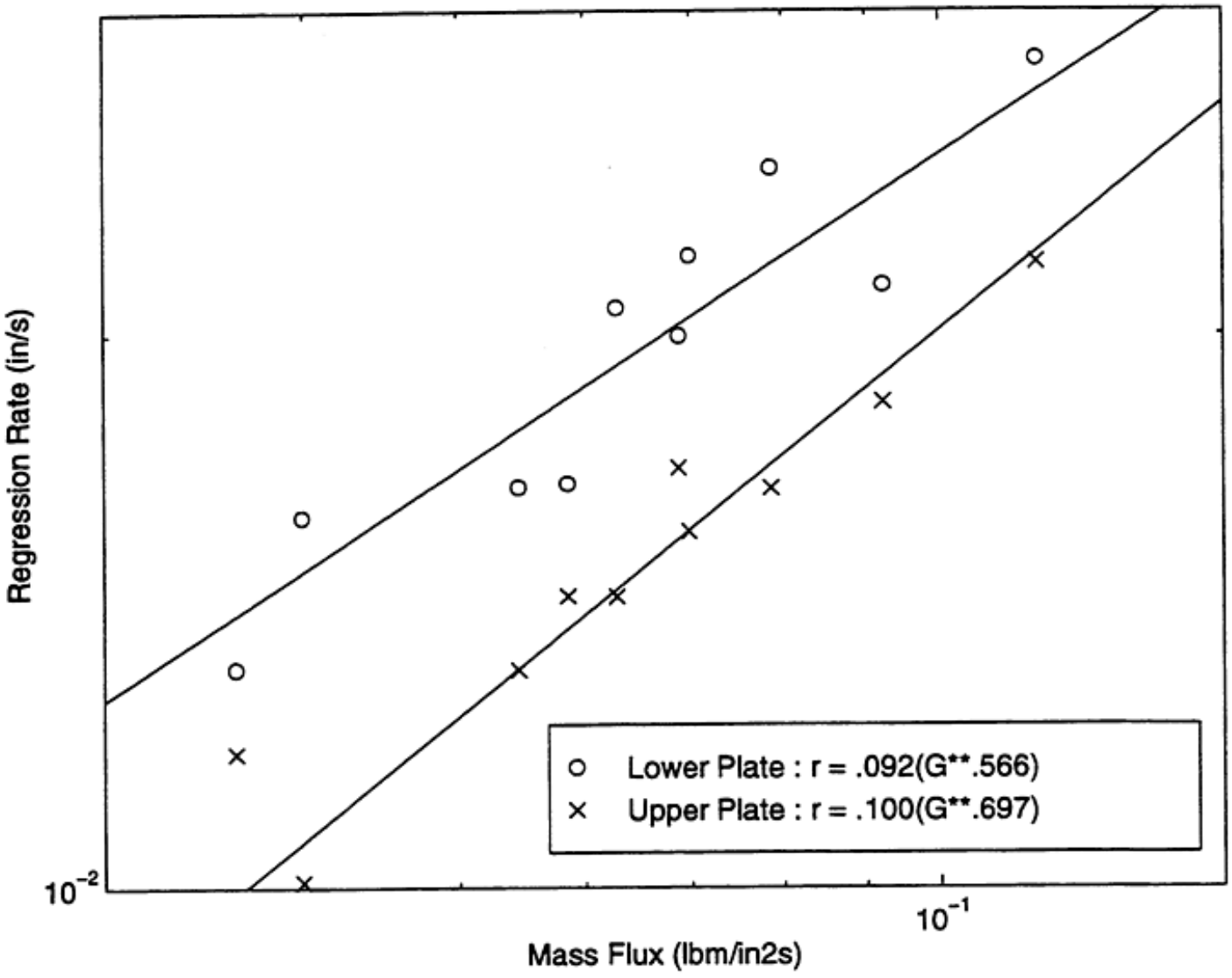

Figure 13: Average Regression Rate vs. Average Total Massflux for Radial-Flow Configuration